Influence of Mathematical Model Comprehensiveness on Distance Protection Setting of Transmission Lines

Igor RAZZHIVIN[1], Julius BAY[1], Anton KIEVETS[1], Alisher ASKAROV[1]

[1]Division for Power and Electrical Engineering, School of Energy and Power Engineering, Tomsk Polytechnic University, Russia

Abstract

The introduction of modern technologies significantly changes the modes of operation of electric power systems (EPS) and has an unpredictable impact on the functioning of relay protection devices (RP), in particular distance protection (DP). It is impossible to adequately measured the impact without detailed modelling of both EPS and RP devices. The subject of this research is the development of a detailed mathematical model of digital distance protection (DDP). When designing such a model, both current and voltage measuring transducers, analogue digital relay protection devices, and digital signal processing were taken into account. In this paper, studies are aimed at assessing the correctness of the third stage of the DP using the detailed and simplified model of the DDP. The operation of the compared models is tested on a 39-bus New England system via MATLAB Simulink simulation data, and a comparative assessment is provided. Such detailed DDP mathematical model in combination with an adequate EPS simulator could be used further for solution of different tasks, such as development, design, analysis, testing and setting of RP algorithms. The article presents the results of preliminary studies of the mentioned problem.

Keywords: relay protection, mathematical modelling, distance protection, electric power system, Simulink modelling

Received: 14 March 2019

To cite this article:
RAZZHIVIN I., BAY J., KIEVETS A., ASKAROV A., "Influence of mathematical model comprehensiveness on distance protection setting of transmission lines", *Electrotehnica, Electronica, Automatica (EEA)*, 2019, vol. 67, no. 1, pp. 54-60, ISSN 1582-5175.

1. Introduction

Currently there are problems in power engineering associated with improper action relay protection and automatics. There are many cases where the wrong action of relay protection led to massive outages and blackouts [1-4]. The consequence of a protection system undesired operation can be extremely serious. Reports and researches on recent blackouts ask for modernization and resetting of existing transmission network relay protection [5-7].

One of the problems caused by incorrect operation of RP is related to the setting of the device. Power system relay protection schemes are generally designed and calculated manually, following standard documents and manufacturer guidelines derived from the long-term experience of power system operation. But this experience is applicable mainly for traditional power systems. Based on these guidelines in the current conditions — the penetration HVDC and FACTS devices, distributed generation, renewables, etc. — it is difficult to state unequivocally whether the RP will function adequately [8-12]. The problem arises, detuning adequate working distance protection in all possible modes, in terms of its correct operation, selectivity, etc.

One of the possible solutions proposed in this article is the use of detailed mathematical models of the main equipment of the power system (generators, transformers, power lines, etc.) and additional equipment (control systems, current transformers, relay protection devices, etc.) in mathematical modelling of EPS for the tasks of setting up and designing RP devices [13-16]. By this approach, it is possible to analyse the influence of the processes occurring in an EPS, on the operation of the relay protection device. In addition, with detailed modelling, it is possible to analyse the trajectories of changes in the measured value and its comparison with the response characteristic of this protection. Information obtained during such studies can be used for improving the RP operation that makes it possible to prevent malfunctioning, so that the cascaded line tripping is avoided.

The article discusses the impact of the processes occurring in the EPS on distance protection. Distance approach is the common method for both primary and backup protection of transmission lines. Though a distance relay is set to protect a line from any type of faults, modes in EPS may occur in which the DP, in particular the third stage, can work wrong, for example, with a large scale disturbance, in the power swing mode or network overload [17]. The principle of DP is based on the control of resistance, which is formed from the values of voltages and currents. To obtain an accurate value of resistance in the current mode, it is important to set up digital filters, which not only determine the value of the main parameters of the voltage and current signal, but also should take into account the saturation of the measured values [18, 19].

It should also be noted that in this paper for modelling digital DDP device incorporates many elements that are found in the structure of the DDP devices. In addition, this model is interesting from the point of view of modelling complexity, since the formation of a resistance relay signal takes into account the influence of elements such as a current transformer, a voltage transformer, and various analogue components of a DDP. It should also be noted that in the simulation were used modern ideas about the

methods of digital data processing and algorithms for swings blocking device [20-25].

2. Simulation model

For the study, a model that includes the following elements: an electric power system, current and voltage transformers, and a relay protection device has been developed.

The relay protection device in its structure has analogue and digital parts Figure 1.

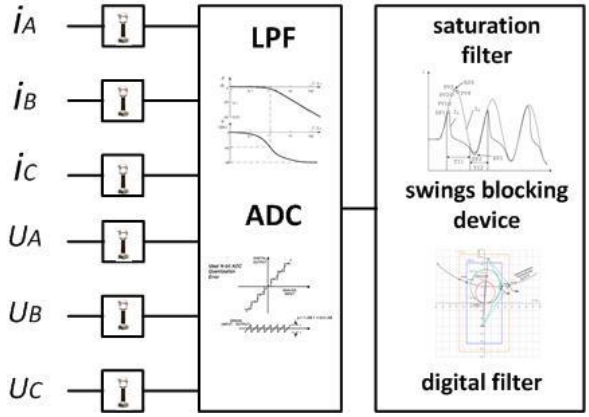

Figure 1. A block diagram of a relay protection device

In the analogue part intermediate current and voltage transformers, a second-order active low-pass filter and an analogue-to-digital converter (ADC) are presented. The digital part includes determining the saturation signal filter, the digital filter, determining the signal parameters and the swings blocking device.

2.1. Electric power system model

Test models of EPS are often used in research activities, since, unlike the models of real systems, the initial parameters of generators, lines and loads are precisely defined or specified. Also scripting calculations are not hindered by the lack of statistical data and the EPS dynamics. The 10-Machine New-England Power System (IEEE-39 Bus test system) was chosen as the model of the electric power system, most often the scheme is applicable in the study of steady-state and dynamic stability. The test EPS is free available for research and educational purposes, the parameters for this system are taken from [26-27].

The IEEE 39-bus modified test system contains 49 buses, 32 transmission lines, 24 transformers and 10 generators. It has 19 constant impedance loads totalling 6097.1 MW and 1408.9 MVAr. Figure 2 shows the part of the power system for which the study was conducted.

2.2. Mathematical models of analogue elements

As analogue elements in the model are: intermediate current and voltage transformers [28], active second-order low-pass filter, current-to-voltage converter, voltage converter and ADC.

2.2.1. Mathematical model of current transformer

The processes of operation of a current transformer (CT) [28] are described by a system of equations:

$$\begin{cases} w_2 S\frac{dB}{dt} = (R_2 + R_b)i_2 + (L_2 + L_b)\frac{di_2}{dt} \\ Hl = w_1 i_1 - w_2 i_2 \\ B = f(H) \end{cases} \quad (1)$$

where: R_2, L_2 is the resistance and inductance of the secondary winding; S — steel section of the magnetic circuit; L is the average length of the magnetic field line; i_1, i_2 — primary and secondary currents CT; w_1, w_2 — the number of turns of the primary and secondary windings, respectively; B = f(H) is the magnetization characteristic of electrical steel.

Transformer iron core saturation modelling performed by setting the magnetization curve in the form of an approximating function:

$$H = a \cdot \sinh(b \cdot B) + c \cdot B \quad (2)$$

The parameters of equation (2): $a=277\cdot10^{-7}$, b=11.06, c=82.347 were obtained using the Mathcad software package using a set of points of the magnetization curve of CT 3414 (Eh330A) electrical steel.

2.3. Mathematical model of digital filter

The iron core saturation CT is the result: internal, external fault, over-excitation, the influence of inrush currents. These factors can lead to false triggering of RP devices, in order to prevent such situations; they must be identified and compensated. The moment of saturation of the secondary current CT and the main signal parameters, such as the amplitude and phase of the main frequency, are determined by the implemented digital filter using the linear regression method. The negative effect of the iron core saturation is the false triggering of RP devices; in order to prevent such situations; they must be identified and compensated.

The moment of changing the secondary current of CT determination due to the iron core saturation and the main parameters of the signal, such as the amplitude and the phase of the main frequency, occurs due to the implemented digital filter using the linear regression method.

Fault current is described by the equation:

$$i_1(t) = A\sin(\omega t + \varphi) + Be^{-t/\tau} \quad (3)$$

where $i_e(t) = Be^{-t/\tau}$ — the aperiodic component of fault current.

The k-th signal $i_1(t)$ values from 1 to m ($i_1(k)$), $i_1(k+1)$, etc.) were considered, where m is the last point of the unsaturated signal. Meaning:

$$\begin{cases} i_1(k) = b_k + a_k\sin(\omega k\Delta t + \varphi - \varepsilon) \\ i_1(k+1) = b_k e^{-\lambda k} + a_k\sin(\omega k\Delta t + \varphi) \\ i_1(k+2) = b_k e^{-2\lambda k} + a_k\sin(\omega k\Delta t + \varphi + \varepsilon) \\ i_1(k+3) = b_k e^{-3\lambda k} + a_k\sin(\omega k\Delta t + \varphi + 2\varepsilon) \end{cases} \quad (4)$$

where k = 1, 2, ..., m is the coefficient of the main frequency; a_k, b_k are the coefficients of the aperiodic component of the signal; ω — frequency and ωkΔt+φ-ε — the initial phase of each k-th point, respectively; ε=ωTs and λ=Δt/τ, where Ts is the sampling period of the signal $i_1(t)$, τ — is the time constant of the exponential component.

In system (4), the values $i_1(k)$, $i_1(k+1)$, $i_1(k+2)$, $i_1(k+3)$ are obtained from the ADC. To determine the unknown components $b_k e^{-\lambda k}$, $bke^{-2\lambda k}$, the expression is used:

$$\begin{cases} b_k e^{-\lambda k} = \frac{i_1(k+2) - 2i_1(k+1)\cos\varepsilon + i_1(k)}{2(1-)\cos\varepsilon} \\ b_k e^{-2\lambda k} = \frac{i_1(k+3) - 2i_1(k+2)\cos\varepsilon + i_1(k+1)}{2(1-)\cos\varepsilon} \end{cases} \quad (5)$$

The aperiodic component obtained from the system of equations (5)

$$i_e(g) = b_k e^{-\lambda k}(e^{-\lambda k})^{g-(k+1)} \quad (6)$$

where $e^{-\lambda k}$ is defined as $bke\text{-}2^{\lambda k}$/ $b_k e^{-\lambda k}$, and g = 1, 2, ...,n, therefore the component of the periodic signal (main frequency) of each selected point can be obtained through:

$$i_f(k) = i_1(k) - i_e(k) \quad (7)$$

To improve the accuracy of calculation of the exponential component of fault current values should be averaged by the following formula:

$$\begin{cases} e^{-t/\tau} = \frac{1}{(m-3)}\sum_{k=1}^{m-3} e^{-\lambda k} \\ B = \frac{1}{(m-3)}\sum_{k=1}^{m-3} \frac{b_k}{(e^{-\lambda k})^{k\Delta t}} \end{cases} \quad (8)$$

The solution to the problem of finding the aperiodic component is performed by using the Matlab Simulink. To determine the accuracy of the solution, the aperiodic part of the input signal was compared with the result of the digital filter operation.

Comparison shows that the part of the simulated digital filter rather accurately determines the aperiodic component of the fault current. The parameters of the periodic component were determined by linear regression, namely the recursive least squares method (LS method). The periodic part of the signal is determined by:

$$i_f(k) = a_1 sin(\omega k\Delta t) + a_2 cos(\omega k\Delta t) \quad (9)$$

To apply the recursive LS method, equation (9) must be transformed in order to minimize the squared residual *s*:

$$s(a) = \sum_{i=1}^{n}(r_i(a))^2 \quad (10)$$

where *n* and *s(a)* are the number of selected values and the required function, respectively;

$r_i(a)=i_f(k)-(a_1\sin(\omega k\Delta t)+a_2\sin(\omega k\Delta t))$ — the difference between the actual value of the sample and the values of the functions of the model.

$$f(a) = i_f - L \cdot a \quad (11)$$

where

$$f(a)^T = [r_1(a),\ r_2(a) \dots\ r_m(a)]^T \quad (12)$$

$$i_f = [i_f(1),\ i_f(2) \dots\ i_f(m)] \quad (13)$$

$$L = \begin{bmatrix} \sin(\omega\Delta t) & \cos(\omega\Delta t) \\ \sin(2\omega\Delta t) & \cos(2\omega\Delta t) \\ \dots & \dots \\ \sin(m\omega\Delta t) & \cos(m\omega\Delta t) \end{bmatrix} \quad (14)$$

Based on formulas (13) (14), the objective function was transformed into a matrix form:

$$\mathrm{s(a)} = \mathrm{(a)^T f(a)} \quad (15)$$

Value of the vector a:

$$a = (L^T L)^{-1} L^T i_f \quad (16)$$

Components of the main frequency signal obtained by deriving the square root of the sum of squares of coefficients at each sampling point.

$$A = \sqrt{a_1^2 + a_2^2} \quad (17)$$

$$\varphi = atan(\frac{a_1}{a_2}) \quad (18)$$

The saturation of the CT magnetic circuit can lead to false triggering of the relay protection devices. In the case of distance protection, this may lead to a delayed response when the resistance value zone is changed, the resistance value is overestimated by the DP response characteristics; To determine the iron core saturation CT, the method of determining the unsaturated portion of the signal of the secondary current CT was used by estimating the stability of the filter, which determines the amplitude of the signal.

The average deviation of the determined amplitude of the secondary current CT, depending on the effective value of the amplitude, is the main indicator of the stability of the filter. Thus, the normalized average deviation (NAD) of the last eight amplitude values [5] is used as an output indicator of the filter stability and is defined as:

$$NAD = \frac{(\frac{1}{8}\sum_{i=-7}^{0}|M_i - \bar{M}|)}{\bar{M}} \quad (19)$$

$$\bar{M} = \frac{1}{8}\sum_{i=-7}^{0} M_i \quad (20)$$

where, M_i, i=-7, -6, ..., 0 the last 8 values of the signal amplitude.

In the case of a sinusoidal signal, the value of NAD takes the value 0, therefore, such areas can be determined when the value of NAD is lower than a certain value.

However, the results of studies [5] showed that the secondary current CT has a sinusoidal form not only in the unsaturated state, but also at the saturation, this phenomenon is observed due to the linearity of the core characteristics at the high excitation currents due to the constant inductance of the air gap of CT (Figure 2).

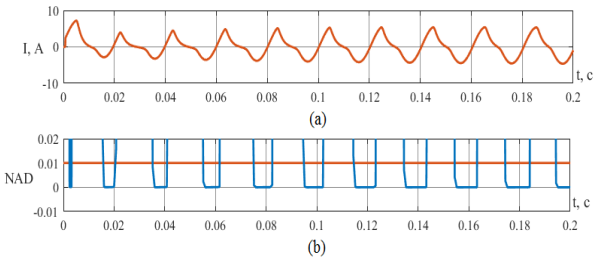

Figure 2. (a) Secondary current of saturated CT; (b) NAD signal and level of comparison 0.01

Therefore, the value of NAD falls below a certain value in the following cases:

1) CT is not saturated in the normal mode;
2) CT is not saturated in the fault mode;
3) the CT is saturated in the fault mode, and a part of the sample is an unsaturated sample of the secondary current of the CT;
4) The CT is saturated in the fault mode, and a part of the sample is a saturated part of the secondary CT current.

Thus, the selection of the signal of the secondary current will be unsaturated if one of the following conditions is met:

1) NAD <0.01 and M0 <2IN and T_{low}> 20 ms — case 1;
2) NAD <0.01 and M0> 2IN — case 2 or 3 and the secondary current is saturated or slightly distorted when one of these conditions is met;
3) NAD <0.01 and M0 <2IN and T_{low}>20 ms — case 4;
4) NAD> 0.01 — the signal is saturated or distorted.

where: T_{low} the time interval at which the condition M0<2IN; IN — secondary current CT.

2.4. The second order low pass filter

In the Matlab software package, a low-pass filter was implemented with a transfer function:

$$\frac{V_{out}(s)}{V_{in}(s)} = \frac{\frac{1}{R_1C_1R_2C_2}}{s^2+s\left(\frac{1}{R_1C_1}+\frac{1}{R_2C_2}\right)+\frac{1}{R_1C_1R_2C_2}} \quad (21)$$

As the cut-off frequency, a frequency of 500 Hz was chosen [28]. For a given frequency, the parameters of the circuit were calculated, as well as the corresponding coefficients of the function (5). The filter worked with a voltage consisting of a signal of the main frequency with an amplitude of 20 and a frequency of 1000 Hz with an amplitude of 2. The obtained Characteristic confirms the correctness of the filter operation.

2.5. Analogue-to-digital converter

To realize an analogue-to-digital converter (ADC), it was decided to realize a sigma-delta modulator [28]. This ADC is a simple tracking system: the voltage at the integrator output "monitors" the input voltage. The result of the operation of this scheme in conjunction with a low pass filter is a bit-stream. Next, the modulator is combined with the "decimation filter".

The operation of this ADC with a signal having both aperiodic and periodic components was examined. The result shows that the signal is quantized by value and time, which is the result of the sigma-delta ADC operation.

2.6. A mathematical model of the swings blocking device

In the event of a power swing, the measured resistance may move from the area of normal load to the area of the characteristic of the distance protection set point, which may lead to its inadvertent operation. For example, in the United States, in 2003, a serious accident occurred, the cause of which was triggered by the third DP level due to overload and power swings, which resulted from the loaded state of the power system, which led to system outages [20]. In article [17], a method of a swings blocking applying, which is based on the prediction of the time of a change in the rotor angle of a synchronous generator from a set of measured data, obtained in real time after the occurrence of a fault or other disturbance.

In Matlab Simulink, models of swing locking devices were implemented. The result of the turn lock operation is presented in the case study.

3. Results and discussion

Within the framework of the studied fragment of the power system, distance protection of type ShE 2607 021 from EKRA was selected.

EKRA (Research and Production Enterprise Ltd.) performs: research and advanced development activities, design works, adjustment supervision of equipment at site, training, warranty maintenance and service maintenance. EKRA manufactures microprocessor-based protective relaying and control cubicles for 6–1200 MW power stations and 6–750 kV substations; emergency control cubicles; Automatic Process Control for substations; operating DC voltage systems, etc.).

The parameters for the response characteristics of the third-stage DDP were determined according to [30]. This level of protection should ensure reliable disconnection of all types of faults along the entire length of the line, as well as redundancy damage to adjacent connections. The third stage is adjusted from the minimum resistance in the operating mode [30].

To calculate the set point of the third stage R3 resistance, the following expression [30] is generally used:

$$R_3 = R_{calc} + R_{tr} \quad (22)$$

where R_{calc} is the calculated active resistance of the third-stage protection, R_{tr}=R_{arc} is the active transient resistance of the arc at the line damage site during phase-to-phase fault. In turn:

$$R_{tr} = U_{arc}\frac{l}{I} \quad (23)$$

where l is the arc length (m), defined as the distance between the phase conductors (or, when short to ground, between the wire and the support), I — is the minimum current (A) flowing from the protection installation site to the fault point at the end of the sensitivity zone of the first steps of distance protection. U_{arc}=1050 V/m according to [30].

The setting for the reactive component of the resistance is determined according to [30]:

$$X_3 = K_{off} * X_{calc} \quad (24)$$

where K_{off} — the coefficient of offset from the *fault*, equal to 0.85, X_{calc} — the calculated inductive resistance of the third stage of protection.

Based on expressions (33), (34), as well as expressions (35), we have the following:

$$R_{tr} = U_{arc}\frac{l}{I} = 2500 \cdot \frac{10}{1761} = 14.2 \text{ Ohm}$$

$$R_{arc} = 1050 \cdot \frac{10}{1438} = 7.3 \text{ Ohm}$$

$$R_3 = R_{calc} + R_{tr} = 101.2 + 14.2 = 115.4 \text{ Ohm}$$

$$R_z = 66.2 + 7.3 = 73.5 \text{ Ohm}$$

$$X_3 = 0.85 \cdot 193.2 = 164.22 \text{ Ohm}$$

$$X_z = 0.85 \cdot 130.1 = 110.6 \text{ Ohm}$$

where l the value is taken from [35], I — the value obtained using simulation in Matlab Simulink, R_{calc}, X_{calk} — calculated according and angles of inclination are taken from [30].

The protection operation with three types of short-circuit protection is modelled — three-phase, double line-to-ground and line-to-line faults.

A. Case 1. Three phase fault

When a three-phase fault occurs, the hodograph of resistances in both *cases* (using a simplified and accurate DP model) behaves almost the same, both for the short-range (Figure 3a) and for the far (Figure 3b) of the reservation. This is due to the fact that three-phase faults are symmetrical faults, however secondary equipment records DP only leads to a more accurate determination of the resistance of the vector (keeping CT saturation, signal filtering).

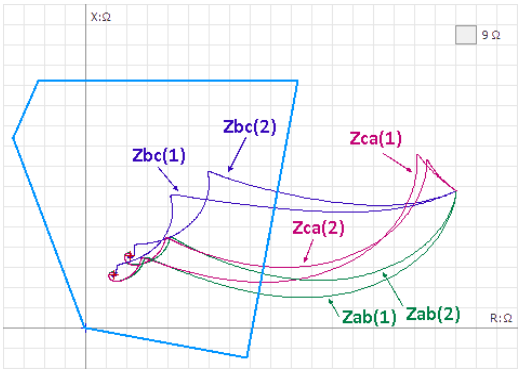

(a)

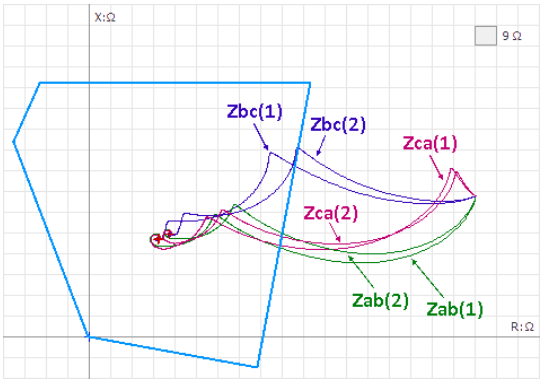

(b)

Figure 3. Near (a) and far (b) reservations: hereinafter, the index (1) is a simplified model of DP, (2) is a detail model of DP

With a symmetric three-phase fault with near-reservation (Figure 3a), the parameters of the resistance lines:

- the simplified model: Zab(1) = Zbc(1) = Zca(1) = 12.8 + j23.7 Ohm;
- the exact model: Zab(2) = Zbc(2) = Zca(2) = 19.1 + j31 Ohm;

The relative error δ of the experimental result of the simplified model with respect to the exact was 26 %.
With long-distance redundancy (Figure 3b):

- the simplified model: Zab(1) = Zbc(1) = Zca(1) = 27.4 + j42.5 Ohm;
- the exact model: Zab(2) = Zbc(2) = Zca(2) = 34 + j44.3 Ohm.

The relative error δ of the experimental result of the simplified model with respect to the exact was 9.5 %.

Resistance hodographs are included in the zone of operation, the DP model works reliably in all cases. However, the three-phase fault occurs very infrequently in the power systems (only 3-5 % of all system faults), therefore, the double line-to-ground and line-to-line faults are of a greater practical interest in considering the behaviour of the resistance hodographs with asymmetric faults.

B. Case 2 – Double line-to-ground faults

Constructed resistivity hodographs for the near-redundancy are included in the zone of operation (operating characteristic) - the DP model works reliably (for a DP, a sufficient condition for the operation is that two resistance vectors fall into the zone of operation). In the case of long-distance redundancy, a completely different picture is observed: with a simplified DP model, the Zab(1) and Zbc(1) vectors also fall within the protection response zone; however, when taking into account the exact DP model, the Zab(2) vector is located near the boundary of the trigger zone, and the Zbc(2) vector is outside this zone (Figure 4a-b). Thus, it turns out that the traditional setting does not ensure the correct functioning of the DP in this mode.

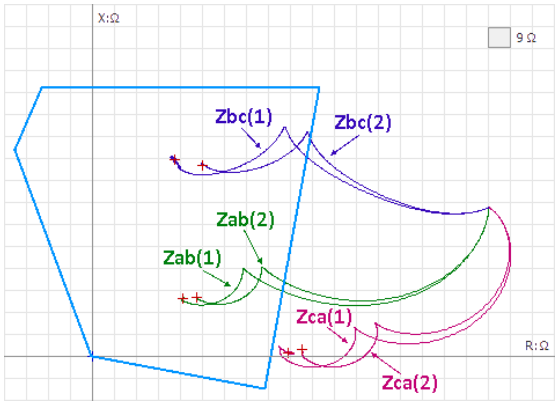

(a)

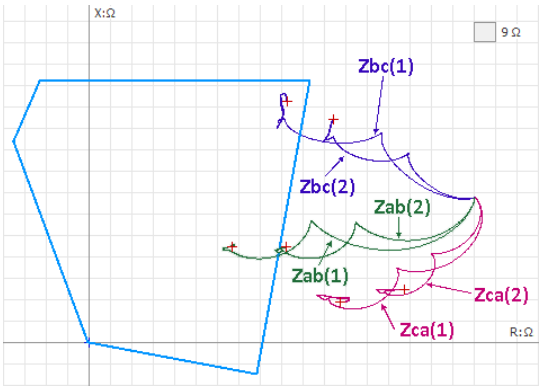

(b)

Figure 4. Near (a) and far (b) reservations

With a Double line-to-ground fault with a near reservation (Figure 4a), the parameters of the resistance lines:

- the simplified model: Zab(1) = 37.3 + j22.3 Ohm; Zbc(1) = 34.8 + j83.4 Ohm; Zca(1) = 79.2 + j2 Ohm;
- exact model: Zab(2) = 43.9 + j23.8 Ohm; Zbc(2) = 45 + j81.8 Ohm; Zca(2) = 86.3 + j3.2 Ohm.

With long-distance redundancy (Figure 4b):

- the simplified model: Zab(1) = 59.8 + j43.2 Ohm; Zbc(1) = 81.1 + j102.1 Ohm; Zca(1) = 106.1 + j18 Ohm;
- the exact model: Zab(2) = 82 + j42.6 Ohm; Zbc(2) = 103.7 + j93.8 Ohm; Zca(2) = 135 + j23.8 Ohm.

C. Case 3 - Line-to-line faults

The results of this experiment are shown in (Figure 4a). When taking into account the exact model of remote sensing, the resulting resistance vectors (Zab and Zbc) are either on the border, or outside the zone of the protection operation, and therefore the DDP device may be insensitive to such type of the fault during a typical setting. Based on the foregoing, it is necessary to adapt the existing traditional methods of setting the DP to the specific hardware implementation of digital DP devices.

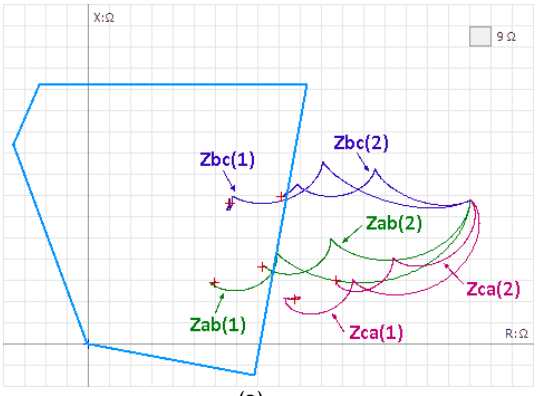

(a)

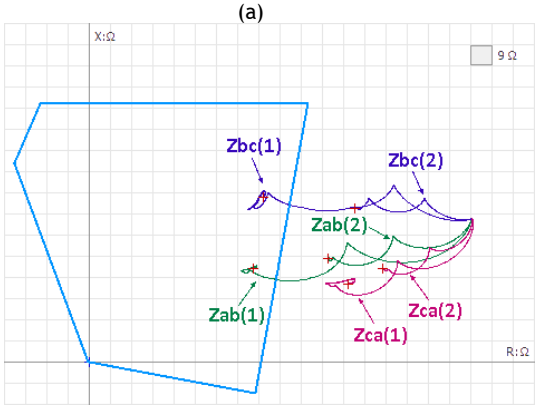

(b)

Figure 5. Near (a) and far (b) reservations

At Line-to-line faults through a transitional resistance with a near-redundancy (Figure 5a), the parameters of the resistance lines:

- the simplified model: Zab(1) = 54 + j24.4 Ohm; Zbc(1) = 59.6 + j59.8 Ohm; Zca(1) = 87.2 + j19.9 Ohm;
- the exact model: Zab(2) = 74.4 + j33 Ohm; Zbc(2) = 81 + j53.8 Ohm; Zca(2) = 106.6 + j27 Ohm;

With long-distance redundancy (Figure 5b):

- the simplified model: Zab(1) = 59.9 + j40.3 Ohm; Zbc(1) = 74.3 + j70.9 Ohm; Zca (1) = 111 + j34.1 Ohm;
- the exact model: Zab(2) = 101.7 + j43.8 Ohm; Zbc(2) = 112.5 + j64.2 Ohm; Zca(2) = 123.2 + j40 Ohm.

4. Conclusions

The article reviewed a detailed mathematical model of DDP taking into account: current and voltage measuring transducers, analogue digital relay protection devices, digital signal processing and blocking from oscillations.

An assessment was made of the correctness of the action of the 3-step level of the DP using the detailed and simplified model of the DDP, using the example of 39-bus New England system via MATLAB Simulink. Such detailed DDP mathematical model in combination with an adequate EPS simulator could be used further for solution of different tasks, such as development, design, analysis, testing and setting of RP algorithms. It has been shown that the use of detailed mathematical models of RP devices is an urgent task. In particular, the authors showed that when designing a RP of EPS, a detailed account is necessary in mathematical models, namely, an account of current transformer saturation, an account of the mathematical model of the swings blocking device. The simulation of the remote RP device was carried out detailed and simplified, the results showed that with near-redundancy in emergency modes, the correct operation of the DDP will be observed, and with long-redundancy - a false positive of the simplified model, while the exact model will work correctly.

5. References

[1] EREMIA, M., SHAHIDEHPOUR, M., Handbook of electric power system dynamics: Modelling, Stability, and Control, Hoboken, NJ, USA: Wiley, 2013, p. 968.

[2] Final Report on 14 August 2003 blackout in the United States and Canada: causes and recommendations. US-Canada Power System Outage Task Force, 2004, viewed on 21 august 2018, retrieved form: https://www3.epa.gov /region1/npdes/merrimackstation/pdfs/ar/AR-1165.pdf

[3] Report of the Enquiry Committee on Grid Disturbance in Northern Region on 30th July 2012 and in Northern, Eastern and North-Eastern Region on 31st July 2012. New Delhi, India, Aug. 16, 2012, viewed on 21 august 2018, retrieved form: http://www.cercind.gov.in/2012/orders /Final_Report_Grid_Disturbance.pdf

[4] ATPUTHARAJAH, A., SAHA, T., "Power system blackouts-literature review", Proceedings of International Conference on Industrial and Information Systems (ICIIS), Sri Lanka, 2009, pp. 460-465.

[5] HOROWITZ, S.H., PHADKE, A.G., "Blackouts and relaying considerations — relaying philosophies and the future of relay systems", IEEE Power Energy Magazine, 2006, vol. 4, no. 5, pp. 60-67, ISSN 1558-4216

[6] SYKES, J., MADANI, V., BURGER, J., ADAMIAK, M., PREMERLANI, W., "Reliability of protection systems (what are the real concerns)", Proceedings of 63rd Annual Conference for Protective Relay Engineers, College Station, TX, 2010, pp. 1-16.

[7] TASDIGHI, M., KEZUNOVIC, M., "Automated Review of Distance Relay Settings Adequacy After the Network Topology Changes," IEEE Transactions on Power Delivery, 2016, vol. 31, no. 4, pp. 1873-1881, ISSN 1937-4208

[8] TELUKUNTA, V., PRADHAN, J., AGRAWAL, A., SINGH, M., SRIVANI, S.G., "Protection challenges under bulk penetration of renewable energy resources in power systems: A review," CSEE Journal of Power and Energy Systems, 2017, vol. 3, no. 4, pp. 365-379, ISSN 2096-0042

[9] NIKOLAIDIS, V.C., TSIMTSIOS, A. M., SAFIGIANNI, A.S., "Investigating Particularities of Infeed and Fault Resistance Effect on Distance Relays Protecting Radial Distribution Feeders With DG," IEEE Access, 2018, vol. 6, pp. 11301-11312, ISSN 2169-3536

[10] JIA, K., GU, C., XUAN, Z., LI, L., LIN, Y., "Fault Characteristics Analysis and Line Protection Design Within a Large-Scale Photovoltaic Power Plant", IEEE Transactions on Smart Grid, 2018, vol. 9, no. 5, pp. 4099-4108, ISSN 1949-3061

[11] WEI, F., LIN, X., LI, Z., CHEN, L., KHALID, M.S., "A New Distance Protection Method Considering TCSC-FCL Dynamic Impedance Characteristics", IEEE Transactions on Power Delivery, 2017, vol. 33, no. 3, pp. 1428-1437, ISSN 1937-4208

[12] PALADHI, S., PRADHAN, A. K., "Adaptive Zone-1 Setting Following Structural and Operational Changes in Power System", IEEE Transactions on Power Delivery, 2018, vol. 33, no. 2, pp. 560-569, ISSN 1937-4208

[13] SENGUPTA, A., MUKHOPADHYAY, S., SINHA, A. K., "Automated Verification of Power System Protection Schemes. Part 1: Modelling and Specifications", IEEE Transactions on Power Delivery, 2015, vol. 30, no. 5, pp. 2077-2086, ISSN 1937-4208

[14] XYNGI, I., POPOV, M., "An Intelligent Algorithm for the Protection of Smart Power Systems", IEEE Transactions on Smart Grid, 2013, vol. 4, no. 3, pp. 1541-1548, ISSN 1949-3061

[15] SUVOROV, A., BOROVIKOV, Y., GUSEV, A., SULAYMANOV, A., ANDREEV, M., RUBAN, N., UFA, R., "Increase in simulation accuracy of self-starting motors used for relay

protection and automatic equipment", Electrical Engineering, 2017, vol. 99, no. 3, pp. 959-968, ISSN 1432-0487
[16] ANDREEV, M., GUSEV, A., SULAYMANOV, A., BOROVIKOV, Y., "Setting of relay protection of electric power systems using its mathematical models", Proceedings of IEEE PES Innovative Smart Grid Technologies Conference Europe (ISGT-Europe), Torino, 2017, pp. 1-6.
[17] SRIRAM, C., KUMAR, D.R., RAJU, G.S., "Blocking the distance relay operation in third zone during power swing using polynomial curve fitting method", Proceedings of International Conference on Smart Electric Grid (ISEG), Guntur, 2014, pp. 1-7.
[18] JI, T.Y., HE, Q., SHI, M.J., LI, M. S., WU, Q.H., "CT saturation detection and compensation using mathematical morphology and linear regression", Proceedings of IEEE Innovative Smart Grid Technologies - Asia (ISGT-Asia), Melbourne, VIC, 2016, pp. 1054-1059.
[19] AJAEI, F.B., SANAYE-PASAND, M., DAVARPANAH, M., REZAEI-ZARE, A., IRAVANI, R., "Compensation of the Current-Transformer Saturation Effects for Digital Relays", IEEE Transactions on Power Delivery, 2011, vol. 26, no. 4, pp. 2531-2540, ISSN 1937-4208
[20] TSIGLER, G. Tsifrovaya distantsionnaya zashchita: printsipy i primenenie [Digital Distant Protection: Principles and Application]. Moscow, Energoizdat, 2005. 322 p. 2
[21] Ch. ROMEIS;M. BILLER; J. JAEGER . «Use of Petri-nets to describe and verify protection system models for time domain simulations» 12th IET International Conference on Developments in Power System Protection, (2014), 14237429/
[22] MÁSLO K., "Distance protection model for network simulators", 14th IEEE Mediterranean Electrotechnical Conference (MELECON 2008), (2008)
[23] MÁSLO K., "Power System Dynamics Modelling", 10th International Conference Control of Power Systems 2012, (2012)
[24] ROMERO J. J., "Blackouts Illuminate India´s Power Problems", IEEE Spectrum 10.12, (2012)
[25] Zhou ZEXIN; Shen XIAOFAN; Zhou CHUNXIA; Wang Shirong; Du Dingxiang. Dynamic simulation inspection test for protection equipment in China, Proceedings. International Conference on Power System Technology. (2002)
[26] IEEE 10 Generator 39 Bus System retrieved form:https://www.researchgate.net/file.PostFileLoader.html?id=55019916f079ed153f8b4598&assetKey=AS%3A273740330405917%401442276188879
[27] PAI Anantha. Energy Function Analysis for Power System Stability. Springer, 1989.
[28] GUREVICH V.I. Mikroprocessornie rele zashity. Ustroistva, problem, perspektivy. – M.: Infra-ingeneria, 2011. – 336c.
[29] "Final Report on the August 14, 2003 blackout in the United States and Canada: causes and recommendations" US - Canada Power System Outage Task Force,2004.
[30] STO 56947007-29.120.70.200-2015. Metodicheskiye ukazaniya po raschotu i vyboru parametrov (ustavok) mikroprotsessornykh ustroystv releynoy zashchity i avtomatiki proizvodstva OOO NPP «EKRA», «ABB», «GE Multilin» i «ALSTOM Grid» / «AREVA» dlya vozdushnykh i kabel'nykh liniy s odnostoronnim pitaniyem napryazh 110-330 kV

Acknowledgments

This work was funded by Ministry of Education and Science of Russian Federation, according to the research project № 14.Y30.18.2379-MC "Investigation of the influence of the spectrum of processes in electric power systems with a significant share of distributed generation and renewable energy sources on the functioning of relay protection devices and the development of a methodology for its adequate setting up"

Biography

Igor RAZZHIVIN was born in Leninogorsk, Kazakhstan in 1989.
He received the M.Sc. in 2015 at Tomsk Polytechnic University.
Currently, he is a Postgraduate of Division for Power and Electrical Engineering, Tomsk Polytechnic University.
He is involved in research work, connected with simulation of renewables.
His research interests concern: Relay protection and renewables
e-mail address: lionrash@tpu.ru

Yuly BAY was born in Tomsk, Russia, in 1991.
He received the Dipl.-Ing. in 2014 at Tomsk Polytechnic University.
Currently he is a Teaching Assistant of Division for Power and Electrical Engineering, Tomsk Polytechnic University.
He is involved in research work, connected with solar cells model development.
His research interests concern: photovoltaic modules modeling, renewable energy sources.
e-mail address: nodius@tpu.ru

Anton KIEVETS was born in Leninsk-Kuzneckiy, Russia, in 1993.
He received the M.Sc. in 2017 at Tomsk Polytechnic University.
Currently, he is a Postgraduate of Division for Power and Electrical Engineering, Tomsk Polytechnic University.
His research interests concern: automation control systems and renewables
e-mail address: kievec.v.l@gmail.com

Alisher ASKAROV was born in Seversk, Russia, in 1994.
He received the M.Sc. in 2018 at Tomsk Polytechnic University.
Currently, he is a Postgraduate of Division for Power and Electrical Engineering, Tomsk Polytechnic University.
He is involved in research work, connected with simulation of automation.
His research interests concern: simulation of automation, control systems and renewables.
e-mail address: aba7@tpu.ru